

Experimental evidence for the Unruh effect

Morgan H. Lynch,^{1,*} Eliahu Cohen,^{2,†} Yaron Hadad,^{3,‡} and Ido Kaminer^{1,§}

¹*Department of Electrical Engineering, Technion: Israel Institute of Technology, Haifa 32000, Israel*

²*Faculty of Engineering and the Institute of Nanotechnology and Advanced Materials,
Bar Ilan University, Ramat Gan 5290002, Israel*

³*Department of Mathematics, University of Arizona, Tucson, AZ, 85721, USA*

(Dated: July 29, 2022)

We examine the radiation emitted by high energy positrons channeled into silicon crystal samples. The positrons are modeled as semiclassical vector currents coupled to an Unruh-DeWitt detector to incorporate any local change in the energy of the positron. In the subsequent accelerated QED analysis, we discover a Larmor formula and power spectrum that are both thermalized by the acceleration. As such, these systems will explicitly exhibit thermalization of the detector energy gap at the celebrated Fulling-Davies-Unruh temperature. Our derived power spectrum, with a nonzero energy gap, is then shown to have an excellent statistical agreement with high energy channeling experiments and therefore provides evidence for the very first observation of the Unruh effect in a non-analogue system.

I. INTRODUCTION

The machinery employed by quantum field theory in curved spacetime [1, 2] to analyze radiation emission has the advantage of stripping away the minute details of the emission process and focusing entirely on the local change in energy of a radiating system. Motivated by the original analyses of Unruh [3] and DeWitt [4] to simplify the transitions in energy of quantum fields in general relativistic backgrounds by modeling them as two level systems, we return to the original use of the “Unruh-DeWitt detector” to analyse how a radiating particle changes its energy. The fundamental insight from this perspective is that for certain deformations in the structure of spacetime, an Unruh-DeWitt detector will undergo a transition, either up or down in energy, and radiate [3–9]. Remarkably, the character of this radiating system will be thermalized at a temperature defined by some characteristic inverse length scale of the spacetime or motion through it, e.g. acceleration, surface gravity, Hubble constant, or some combination thereof, [3, 10–13]. Each of these length scales will define the location of an event horizon which, via quantum fluctuations near the horizon, will emit radiation which is thermalized at that characteristic temperature. In FRW cosmologies [14], signatures of this temperature may be encoded in the anisotropies in the cosmic microwave background [15]. Analogue systems involving “fluid black holes” [16–19] are also capable of exploring not only the temperature, but other properties such as the entropy via correlations between Hawking pairs both inside and outside the effective horizon and even superradiant scattering. The most sought after temperature [20, 21], due to the fact that it appears to be the most readily accessible experimentally, is the acceleration temperature $T = \frac{a}{2\pi}$. The path towards the discovery of this temperature began with the analysis of the quantum mechanical structure of the vacuum in inertial and accelerated reference frames by Fulling [22], the flux of radiation from the 1+1 dimensional moving mirror by Davies [23], and finally by the near horizon examination of Hawking radiation from black holes by Unruh [3]. Understanding this Fulling-Davies-Unruh (FDU) temperature has been the subject of a steadily growing community, as detailed in [20], and the techniques developed to explore it have spread to other fields and fostered their growth as well, e.g. the use of Unruh-DeWitt detectors in relativistic quantum information [24]. This pursuit has culminated in an inherently thermodynamic understanding of the nature of relativistic quantum field theory in classical general relativistic backgrounds [25, 26]. Since the FDU temperature and the general characteristics of electromagnetic radiation are determined by the acceleration, it is through accelerated electromagnetic systems that we expect to see the first signs of accelerated thermality. Here we employ a spacetime formulation of *accelerated quantum electrodynamics* (AQED) [5, 6, 27], via the use of a uniformly accelerated Unruh-DeWitt detector [3, 4] and apply it to high energy channeling radiation [28]. The result of this analysis is a statistically significant indication that *the FDU temperature has finally been observed, in a non-analog experiment.*

*Electronic address: morgan.lynch@technion.ac.il

†Electronic address: eliahu.cohen@biu.ac.il

‡Electronic address: yaronhadad@gmail.com

§Electronic address: kaminer@technion.ac.il

We demonstrate that a nonzero Unruh-DeWitt detector energy gap, which encodes local changes in energy of the radiating electron or positron, will not only be thermalized at the FDU temperature but also provide a significantly better explanation of high energy channeling radiation than conventional models. We present the AQED response function and compute the power radiated by, and photon power spectrum of, a uniformly accelerated charge current. To compare with the channeling radiation experimental data, we assume an energy gap comprised of a Taylor series in the photon frequency and an acceleration profile based on radiative energy loss. A chi-squared analysis is shown to strongly favor the presence of a non-zero energy gap and therefore provides strong evidence for the observation of thermality at the FDU temperature. Here and throughout, we use natural units $\hbar = c = k_B = 1$.

II. THE AQED RESPONSE FUNCTION AND THERMALIZED ACCELERATED OBSERVABLES

The calculation presented here uses an AQED approach for computing the power radiated from first principles. To this end we make use of the current interaction [29], $\hat{S}_I = \int d^4x \hat{j}_\mu(x) A^\mu(x)$, where $A^\mu(x)$ is the second quantized photon field operator and $\hat{j}_\mu(x)$ is the electron current operator. If we couple an Unruh-DeWitt detector to the current it takes the form $\hat{j}_\mu(x) = u_\mu \hat{q}(\tau) \delta^3(x - x_{tr}(\tau))$. Here u_μ is the four-velocity of the electron and $x_{tr}(\tau)$ is the trajectory of the electron parametrized by its proper time. The monopole moment operator [4] is Heisenberg evolved via $\hat{q}(\tau) = e^{i\hat{H}\tau} \hat{q}(0) e^{-i\hat{H}\tau}$ and the charge of the electron is defined by $q = \langle E_f | \hat{q}(0) | E_i \rangle$, with $|E_i\rangle$ and $|E_f\rangle$ being the initial and final electron energy respectively. Then, by analyzing the amplitude, $\mathcal{A} = i \langle \mathbf{k} | \otimes \langle E_f | \hat{S}_I | E_i \rangle \otimes |0\rangle$, for the electron current to undergo a transition and emit one photon of momentum \mathbf{k} , we can compute the emission rate via the relativistic analogue of Fermi's golden rule. As such, the AQED response function, see Sec. A of the supplementary and [30], is given by

$$\Gamma = q^2 \int d\xi e^{-i\Delta E \xi} U_{\mu\nu}[x', x] G^{\mu\nu}[x', x]. \quad (1)$$

Here we see the standard Fourier transform of the Wightman function, $G^{\nu\mu}[x', x]$, but with indices which, for photons, represent the sum of polarization four-vectors, $\sum_{i,j} \epsilon_i^\mu \epsilon_j^{*\nu}$, which contract with the four-velocity product, $U_{\mu\nu} = u_\mu u_\nu$, to couple the motion to the allowed emission directions. This is nothing more than the byproduct of the standard $v \cdot A$ coupling that one typically sees in electron-photon systems. Recalling the Wightman function is given by the vacuum-to-vacuum two-point function $G^{\nu\mu}[x', x] = \langle 0 | \hat{A}^{\dagger\nu}(x') \hat{A}^\mu(x) | 0 \rangle$, we will have

$$G^{\nu\mu}[x', x] = \frac{1}{(2\pi)^3} \frac{1}{2} \int \frac{d^3k}{\omega} \sum_{i,j} \epsilon_i^\mu \epsilon_j^{*\nu} e^{i(\mathbf{k} \cdot \Delta \mathbf{x} - \omega(t' - t))}. \quad (2)$$

Since we wish to compute the power radiated, \mathcal{S} , we must also include an additional factor of frequency in the above Wightman function [6, 8, 9], as $\mathcal{S} = \int \frac{d\Gamma}{d\omega} \omega d\omega$. When we compute the power radiated by an accelerated electron we should expect to recover the Larmor formula. As we shall see, this is indeed the case. For a trajectory with constant proper acceleration a , parametrized by the proper time τ , we will have hyperbolic motion with four-velocity $u_\mu = (\cosh(a\tau), 0, 0, \sinh(a\tau))$ [20]. Using this trajectory, we arrive at a rather striking result. It is expected that we should obtain the Larmor formula but there is an intermediate result; the fact we have uniformly accelerated motion implies that we should also find signatures of thermality. Explicit computation of the power, see section B of the supplementary, yields

$$\mathcal{S} = \frac{2}{3} \alpha a^2 \frac{1}{1 + e^{2\pi\Delta E/a}}. \quad (3)$$

It is indeed surprising that we have obtained the Larmor formula that is thermalized at the FDU temperature. We must also point out the change in statistics from bosonic to fermionic. This is characteristic of accelerated thermal observables where the statistics depends on, for example, powers of frequency ω in the computation, number of particles emitted, and/or the dimensionality of the system [5, 6, 8, 31]. To recover the standard Larmor formula we must compute the total power by summing over emission and absorption of zero energy Rindler photons [21, 32–34], i.e. $\lim_{\Delta E \rightarrow 0} \mathcal{S}(\Delta E) + \mathcal{S}(-\Delta E) = \frac{2}{3} \alpha a^2$. To compare with experiment we also present the power radiated per unit frequency, see the supplementary Eqs. (S29) and (S30),

$$\frac{d\mathcal{S}}{d\omega} = -i \frac{2}{3} \alpha \frac{\omega^2}{a} e^{-2\pi\Delta E/a} \left[(2\gamma^2 - 1) H_{-\frac{2i\Delta E}{a}}^{(2)} \left(-\frac{2i\omega\gamma}{a} \right) - \frac{1}{2} \left(H_{-\frac{2i\Delta E}{a}+2}^{(2)} \left(-\frac{2i\omega\gamma}{a} \right) + H_{-\frac{2i\Delta E}{a}-2}^{(2)} \left(-\frac{2i\omega\gamma}{a} \right) \right) \right]. \quad (4)$$

Here, $H_\ell^{(2)}(x)$ is the Hankel function of the second kind [35]. We also made the presence of thermality more apparent by making use of the following identity, $H_\ell^{(2)}(x) = e^{i\ell\pi} H_{-\ell}^{(2)}(x)$. The implication of this property of Hankel functions of the

second kind is the manifest detailed balance at thermal equilibrium of the power spectrum by rigorous mathematical identity. The exponent produced by the change in sign of the Hankel index is precisely the Boltzmann factor comprised of the Unruh-DeWitt detector energy gap thermalized at the temperature $T = \frac{a}{2\pi}$. As such, we are led to the conclusion that *systems described by this power spectrum imply the experimental observations of thermality at the FDU temperature.*

This thermal phenomenon, commonly referred to as the Unruh effect [3], has had a considerable amount of effort dedicated to its study as well as a detailed exploration of potential experimental settings which could measure it [20]. The main difficulty with measuring such an effect is the vanishingly small energy scale set by the acceleration when compared to the scale of the energy gap. Broadly speaking, the ability to probe the Unruh effect necessitates $|\Delta E| \sim \frac{a}{2\pi}$ so that the thermal distribution can be explored. The difficulty then lies in bringing the two energy scales together; finding acceleration scales that reach the energy gap from below or energy gaps that can reach the small acceleration scale from above. If both a small energy gap and a large acceleration scale can be found in an experimental system, then this would provide the best chance of measuring the Unruh effect. Through this logic, high acceleration scales coupled to small energy gaps, we apply the above power spectrum, Eq. (4), to the recent channeling radiation experiment in aligned crystals [28]. There we have LHC scale energetic positrons channeled into single crystal silicon (large acceleration) sensitive to the channeling oscillation [36], recoil/radiation reaction [37–41], as well as other processes in the comoving frame (small energy gap). As we shall see, it appears to be the case that channeling radiation may finally enable a system to explore the Unruh effect experimentally.

III. EVIDENCE FOR THE UNRUH EFFECT IN CHANNELING RADIATION

When a highly energetic charged particle propagates in a material, it will lose energy and emit a smooth spectrum of radiation known as bremsstrahlung [42]. This particular process is associated with scattering off individual atomic sites that have a random distribution, i.e. an amorphous crystalline structure for solids or the random distribution of atoms in the case of a liquid or gas. However, if we have a solid with some periodic crystalline structure, then we can look at motion along an axis of symmetry where the charged particle is “channeled” and will propagate in an effective hollow wave guide, or 2-D plane between atomic layers, produced by the structure. Then, the charged particle is confined to the cylindrical potential well and can oscillate back and forth transversely to its direction of propagation and therefore radiate. This process is known as channeling radiation [43]. In the channeling experiment [28], the data from the photon power spectrum produced by the rapidly decelerated positrons is presented and is precisely the observable computed in our analysis. There, daughter products of the LHC proton beam yield 178.2 GeV positrons which are then bent and fired into 3.8 mm and 10 mm samples of amorphous and single crystal silicon.

Under the assumption that channeled particles will lose energy in accordance with radiative energy loss, we expect to see the following differential energy loss, $\frac{dE}{dx} = -\frac{E}{x_0}$ with some effective radiation length x_0 near to that of the measured value specific to the particle and material [44], but slightly modified for the channeling regime. For our purposes, i.e. positrons in silicon, we expect to have a radiation length $x_0 \sim 9.37$ cm. To this end we scale our radiation length via $x_0 \rightarrow \tilde{x}x_0$. Here \tilde{x} characterizes the slightly different radiation length produced by the channeling. Moreover, this energy loss can be used to compute the proper acceleration, $a(\tau)$, as a function of proper time; see Sec. D of the supplementary. Hence, we find

$$a(\tau) = \frac{a_0}{\left(\frac{\tau}{\tau_0} + 1\right)^2}. \quad (5)$$

The acceleration scale is set by the quantity $a_0 = \gamma/x_0$ which is given by the inverse of Lorentz contracted radiation length. The time scale is given by $\tau_0 = \frac{x_0}{\gamma}$. Motions which have a duration of the order of this time scale (or longer) will require a time-dependent analysis. In the present work we will assume that the acceleration is constant, i.e. $a(\tau) = a_0$. We should note that there is indeed sufficient time within the crystal for the acceleration to change by a few percent; the final acceleration a_f compared to the initial a_0 will change by $a_f/a_0 = .98$ and $a_f/a_0 = .92$ for the total travel time of the 3.8 mm and 10 mm crystal respectively. Here, both initial and final accelerations are computed using the scaled radiation length $\tilde{x}x_0$. However, even with this slight time-dependence in the acceleration, we are still ensured of thermality [6].

To compare with the experimental data we need to convert all parameters to GeV [28, 44]; $x_0 \sim 4.75 \times 10^{14}$ GeV⁻¹, $E_0 = 178.2$ GeV, and $m = .000511$ GeV. To model the change in the positron’s energy, we adopt a polynomial energy gap of the form $\Delta E = a_0 + a_1\omega + a_2\omega^2 + a_3\omega^3$; the logic being that the exact expression of the energy difference, produced by the relevant dispersion and conservation of momentum and energy relations associated with all processes present, will be amenable to a Taylor expansion in powers of the emitted photon’s frequency. These parameters will be used to compute the total power spectrum, $\frac{dS_{tot}}{d\omega} = \frac{dS(\Delta E)}{d\omega} + \frac{dS(-\Delta E)}{d\omega}$, with and without the energy gap, and

then compared with the crystal data [28]. In principle, the a_0 term is associated with the channeling oscillation and the $a_2\omega^2$ term is associated with recoil or radiation reaction [37–41]. We also note that the higher power terms, such as recoil $\sim \frac{\hbar^2\omega^2}{2mc^2}$, are necessarily quantum mechanical in nature and thus thermal processes described by such an energy gap will have no classical explanation thereby relieving any ambiguity as to the nature of the effect [45–47]. We included a frequency dependence up to an ω^3 term to capture any further dependence beyond the recoil term since that was what the experiment [28] purported to measure. The energy gap can be “turned off” by setting it to zero. To better match the calculated spectrum to the data we also include an overall scaling factor s to take into account detector efficiencies and other systematics of the experiment, see the methods section for more details. To ensure the presence of thermality we must also examine the emission lifetime. Recalling the emission rate per unit frequency is given by, $\frac{d\Gamma(\omega)}{d\omega} = \frac{d\mathcal{P}(\omega)}{d\omega} \frac{1}{\omega}$, we then invert this and integrate up to a specific frequency to determine the thermalization time for that frequency, i.e. $t(\omega) = \frac{1}{\int_0^\omega \frac{d\Gamma(\omega')}{d\omega'} d\omega'}$. Thermality necessitates that we must have this lifetime be shorter than the travel time within the crystal. This will then require a low frequency cutoff for frequencies that do not have enough time for thermalization to take hold. We then compute best fits of our theory, with respect to the parameters s , \tilde{x} , and a_i , along with the reduced chi-squared statistic for each low frequency cutoff. The plots of our emission lifetime and reduced chi-squared statistics for each cutoff for the 3.8 mm channeling and 10 mm bremsstrahlung crystals [28] are presented in Fig. 1. Also included are the best fit power spectra Eq. (4), and data [28], for both crystals which yielded the first statistically significant signals of accelerated thermality based on the chi-squared statistic. Table 1 contains the computed values of the reduced chi-squared statistic that lie within the one standard deviation boundary, $\chi^2/\nu < 1 + \sqrt{2/\nu}$, for each scenario.

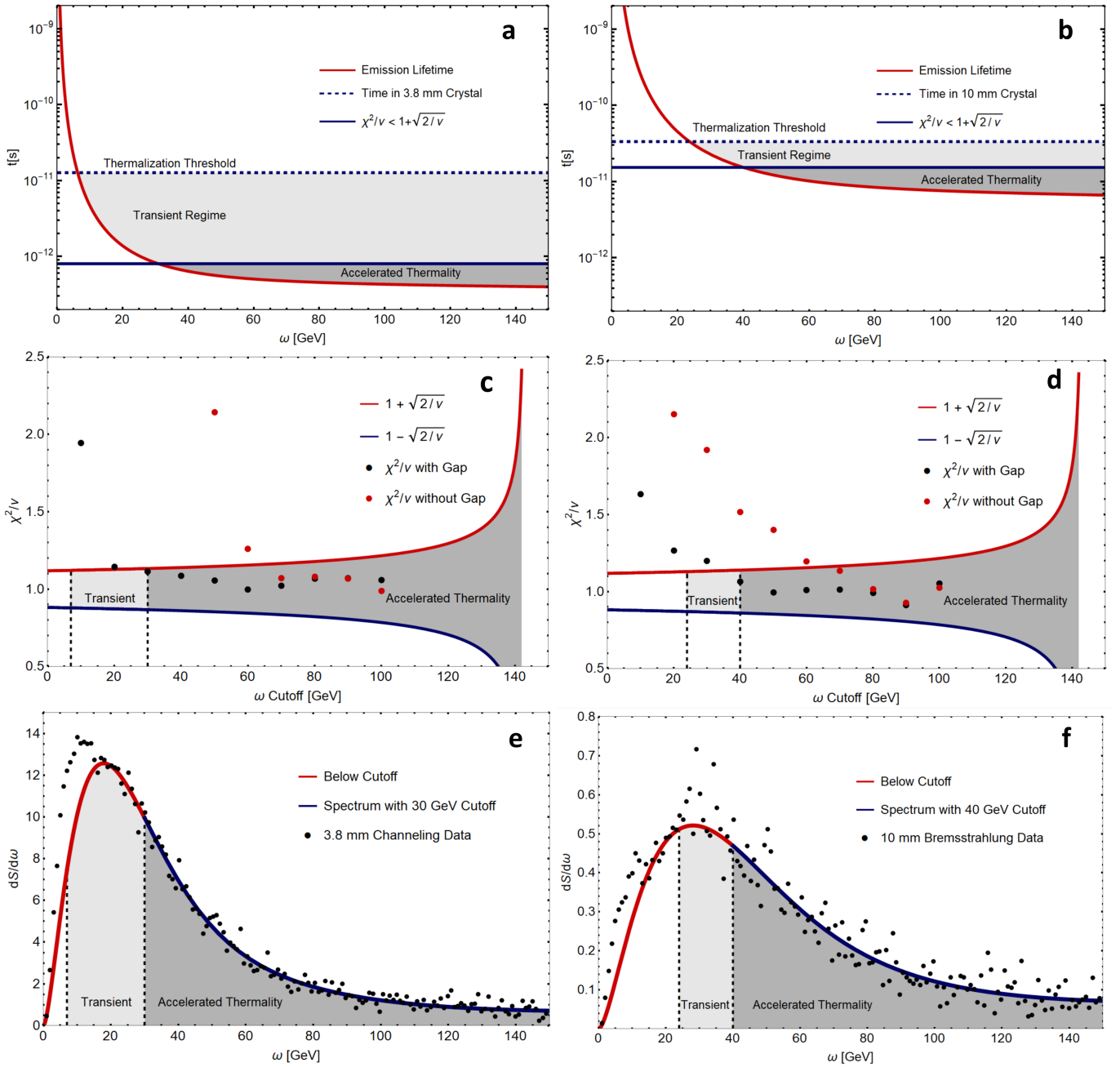


FIG. 1: **Experimental Evidence for the Unruh Effect:** In order for the Unruh effect to manifest itself, whatever process that takes place must have time to thermalize. Plots (a) and (b) show that for the 3.8 mm crystal in the channeling regime and the 10 mm crystal in the bremsstrahlung regime have sufficient time to thermalize. With the threshold of thermality exceeded, we must then look at various cutoffs beyond this threshold for a statistical signal which will confirm it. Plots (c) and (d) show the chi-squared statistic for various low frequency cutoffs. Note that the 3.8 mm channeling radiation and the 10 mm bremsstrahlung both have a $\chi^2/\nu < 1 + \sqrt{2/\nu}$ at 30 GeV and 40 GeV respectively. Note, the presence of a thermalized energy gap is favored over no gap. The implication of this criterion is that the theoretical prediction lies within one standard deviation of all data points. Plots (e) and (f) present the power spectrum with a thermalized energy gap for both crystals with the first cutoffs that satisfy the chi-squared criterion; showing an excellent agreement and thus the first evidence for the observation of the Unruh effect. The best fit parameters and reduced chi-squared statistic for each regime are presented in Table 1.

| Crystal | Energy | Gap | χ^2/ν | $1+\sqrt{2/\nu}$ |
|-----------------|--------|-----|--------------|------------------|
| 3.8 mm Aligned | 30 GeV | No | 4.187 | 1.131 |
| 3.8 mm Aligned | 30 GeV | Yes | 1.114 | 1.133 |
| 10 mm Amorphous | 40 GeV | No | 1.517 | 1.139 |
| 10 mm Amorphous | 40 GeV | Yes | 1.065 | 1.137 |

TABLE I: **Statistical Evidence for Accelerated Thermality:** The reduced chi-squared statistics for our theoretical power spectrum both with and without the energy gap for the 3.8 mm channeling and 10 mm bremsstrahlung samples at the energy where the chi-squared statistic first meets the 1 standard deviation criterion. Our chi-squared statistics show that the data can be rigorously fitted by the power spectrum with the energy gap thermalized at the FDU temperature.

To summarize our analysis, we found sufficient time inside the 3.8 mm and 10 mm crystals for the system to be thermalized by the acceleration. The thermalization time implied a low energy cutoff of ~ 7 GeV and ~ 24 GeV for the 3.8 mm channeling and 10 mm bremsstrahlung data respectively. Performing best fits of our theory to the data, with cutoffs at multiples of 10 GeV, yielded a reduced chi-squared statistic within the 1 standard deviation threshold at 30 GeV and 40 GeV for the 3.8 mm and 10 mm crystals respectively. The overall chi-squared statistic also favors a nonzero energy gap with differences, $\Delta\chi^2 = |\chi_{gap}^2 - \chi_{no\ gap}^2|$, given by $\Delta\chi_{3.8}^2 = 364$ and $\Delta\chi_{10}^2 = 52.6$. The theory employed in the analysis obeys detailed balance, is thermalized at the FDU temperature, and also reproduces the Larmor formula in the appropriate limit [21, 32–34]. It is through these multiple sanity checks and figures of merit that we are led to the conclusion of accelerated thermality.

The main focus of this manuscript dealt with the presence of the Unruh effect in a high energy channeling radiation experiment that purported to measure radiation reaction [28]. However, there are two additional experiments that also report evidence of radiation reaction using plasma wakefield acceleration [48, 49]. There, rather than the photon power spectrum, the final state electron energy was measured. It would be an interesting avenue of research to apply this formalism to their experiments in search of accelerated thermality as well. The connection to between the Unruh effect and radiation reaction has long been discussed in the literature [50, 51] and it appears that these, and future, systems may provide a robust experimental setting to explore these intriguing aspects of radiation simultaneously.

IV. CONCLUSIONS

In this article, we have presented the theory of accelerated quantum electrodynamics and used it to explore the radiation produced by uniform accelerated motion. When applied to the problem of channeling radiation we are able to incorporate a local change in energy, utilizing techniques from quantum field theory in curved spacetime, by setting the energy gap of an Unruh-DeWitt detector equal to a general polynomial in the emitted photons frequency thereby connecting it with the Unruh effect. This work not only explores channeling radiation, in a quantitative manner, but also sheds new light on it and the Unruh effect in a manner that is backed by the experimental evidence. Our theory and analysis indicate that *the recent high energy channeling radiation experiment has a significant statistical signal for the first observation of thermalization at the Fulling-Davies-Unruh temperature and thus the first observation of the Unruh effect.*

V. METHODS

To generate all figures, our power spectrum was scaled by $s\frac{3x_0}{4c}$ and the radiation length was scaled by $x_0 \rightarrow \tilde{x}x_0$ except in the prefactor for $\frac{3x_0}{4c}$. This scaling factor is included in our analysis since it is used by the experimental group [28] to take into account the detectors signal conversion process to ensure a single photon spectrum. We scaled the radiation length by a factor of \tilde{x} to take into account any additional phenomena that may occur at such high energies such as pair creation [44] and the strong transverse channeling oscillations [36] which contribute to the energy loss and subsequent deceleration. The energy gap was given by a general polynomial of the form $\Delta E = a_0 + a_1\omega + a_2\omega^2 + a_3\omega^3$. Then we performed a least squares best fit to obtain the values for our six parameters s , \tilde{x} , and a_i . In the case of no energy gap we merely set $\Delta E = 0$. To directly compare to the crystal data [28], our spectrum was multiplied by the factor of $\frac{3x_0}{4c} = 2.34 \times 10^{-10}$ s. This means the power spectrum we plot is $\frac{dS}{d\omega} \rightarrow s\frac{3x_0}{4c} \frac{dS}{d\omega}$. Note, here we explicitly put in the speed of light. This scaling of the radiation length *is not* included in the scale factor $\frac{3x_0}{4c}$ since the experimental

analysis did not include it. We must also note that although our computation was carried out in the rest frame of the electron, it was also carried out at $\Delta x = 0$, see Sec. C of the supplementary material. This is equivalent to performing the calculation at $\beta = 0$, and therefore we need to boost the positron to the LHC beam energy. As such our acceleration must be boosted via $a \rightarrow a\gamma^3$ along with an overall factor of γ to boost the power spectrum itself. We then plot our power spectrum with the best fit parameters for each case. To compute the chi-squared statistic, we evaluated our best fit power spectra at the x-value of each data point to compare the theoretical y-value to the data. The chi-squared per degree of freedom is then given by $\chi_{the}^2/\nu = \sum_i \frac{(y_{the}(x_{exp}^i) - y_{exp}^i)^2}{\sigma_i^2}$. Here i labels the data points and σ_i is the experimental error of each data point. The number of degrees of freedom is given by $\nu = n - p$, with $n = 150$ and $p = 6$ and $p = 2$ is the number of fit parameters for the power spectrum with and without the energy gap respectively.

-
- [1] L. Parker, *The Creation of Particles by the Expanding Universe*, Ph.D. thesis, Harvard University, (1966).
- [2] L. Parker, *Thermal radiation produced by the expansion of the Universe*, *Nature* **261**, 20 (1976).
- [3] W. G. Unruh, *Notes on black-hole evaporation*, *Physical Review D* **14**, 870 (1976).
- [4] S. Hawking, W. Israel, and B. S. DeWitt, *General Relativity an Einstein centenary survey*, (Cambridge University Press, Cambridge, 1979).
- [5] M. H. Lynch, *Acceleration-induced scalar field transitions of n-particle multiplicity*, *Physical Review D* **90**, 024049 (2014).
- [6] M. H. Lynch, *Accelerated quantum dynamics*, *Physical Review D* **92**, 024019 (2015).
- [7] R. Muller, *Decay of accelerated particles*, *Physical Review D* **56**, 953 (1997).
- [8] G. E. A. Matsas and D. A. T. Vanzella, *Decay of protons and neutrons induced by acceleration*, *Physical Review D* **59**, 094004 (1999).
- [9] D. A. T. Vanzella and G. E. A. Matsas, *Decay of accelerated protons and the existence of the Fulling-Davies-Unruh effect*, *Physical Review Letters* **87**, 151301 (2001).
- [10] S. W. Hawking, *Black hole explosions?* *Nature* **248**, 30 (1974).
- [11] G. W. Gibbons and S. W. Hawking, *Cosmological event horizons, thermodynamics, and particle creation*, *Physical Review D* **15**, 2738 (1977).
- [12] M. H. Lynch and N. Afshordi, *Temperatures of renormalizable quantum field theories in curved spacetime*, *Classical and Quantum Gravity* **35**, 225008 (2018).
- [13] A. Dhumuntarao, J. T. G. Gherzi, and N. Afshordi, *Instantaneous temperatures la Hadamard: Towards a generalized Stefan-Boltzmann law for curved spacetime*, arXiv:1804.05382 [gr-qc], (2018).
- [14] N. Obadia, *How hot are expanding universes?* *Physical Review D* **78**, 083532 (2008).
- [15] I. Agullo and L. Parker, *Non-Gaussianities and the stimulated creation of quanta in the inflationary universe*, *Physical Review D* **83**, 063526, (2011).
- [16] W. G. Unruh, *Experimental black-hole evaporation?*, *Physical Review Letters* **46**, 1351 (1981).
- [17] S. Weinfurter, E. W. Tedford, M. C. J. Penrice, W. G. Unruh, and G. A. Lawrence, *Measurement of stimulated Hawking emission in an analogue system*, *Physical Review Letters* **106**, 021302 (2011).
- [18] J. R. M. de Nova, K. Golubkov, V. I. Kolobov, and J. Steinhauer, *Observation of thermal Hawking radiation at the Hawking temperature in an analogue black hole*, arXiv:1809.00913 [gr-qc], (2018).
- [19] L.-P. Euve', F. Michel, R. Parentani, T.G. Philbin, and G. Rousseaux, *Observation of noise correlated by the Hawking effect in a water tank*, *Physical Review Letters* **117**, 121301 (2016).
- [20] L. C. B. Crispino, A. Higuchi, and G. E. A. Matsas, *The Unruh effect and its applications*, *Review of Modern Physics*, **80**, 787 (2008).
- [21] G. Cozzella, A. G. S. Landulfo, G. E. A. Matsas, and D. A. T. Vanzella, *Proposal for observing the Unruh effect using classical electrodynamics*, *Physical Review Letters* **118**, 161102 (2017).
- [22] S. A. Fulling, *Nonuniqueness of canonical field quantization in Riemannian space-time* *Physical Review D* **7**, 2850 (1973).
- [23] P. C. W. Davies, *Scalar production in Schwarzschild and Rindler metrics*, *Journal of Physics A: Mathematical and General* **8**, 609 (1975).
- [24] B. L. Hu, S.-Y. Lin, and J. Louko, *Relativistic quantum information in detectors-field interactions*, *Classical and Quantum Gravity* **29**, 224005 (2012).
- [25] J. D. Bekenstein, *Black holes and entropy* *Physical Review D* **7**, 2333 (1973).
- [26] T. Jacobson, *Thermodynamics of spacetime: The Einstein equation of state*, *Physical Review Letters* **75**, 1260 (1995).
- [27] M. H. Lynch, E. Cohen, Y. Hadad, and I. Kaminer, *Accelerated-Cherenkov radiation and signatures of radiation reaction*, *New Journal of Physics* **21**, 083038 (2019).
- [28] T. N. Wistisen, A. D. Piazza, H. V. Knudsen, and U. I. Uggerhoj, *Experimental evidence of quantum radiation reaction in aligned crystals*, *Nature Communications* **9**, 795 (2018).
- [29] M. E. Peskin and D. V. Schroeder, *An Introduction to Quantum Field Theory*, (CRC Press, Boca Raton, 1995).
- [30] N. D. Birrell and P. C. W. Davies, *Quantum Field Theory in Curved Space*, (Cambridge University Press, Cambridge, 1982).
- [31] S. Takagi, *Vacuum noise and stress induced by uniform acceleration: Hawking-Unruh effect in Rindler manifold of arbitrary*

- dimension*, Progress in Theoretical Physics Supplement **88**, 1 (1986).
- [32] A. Higuchi, G. E. A. Matsas, and D. Sudarsky, *Bremsstrahlung and Fulling-Davies-Unruh thermal bath*, Physical Review D **46**, 3450 (1992).
- [33] H. Ren and E. J. Weinberg, *Radiation from a moving scalar source*, Physical Review D **49**, 6526 (1994).
- [34] M. Pauri and M. Vallisneri, *Classical Roots of the Unruh and Hawking Effects*, Foundations of Physics **29**, 1499 (1999).
- [35] M. Abramowitz and I. Stegun, *Handbook of Mathematical Functions*, (National Institute of Standards and Technology, Washington D.C., 1964).
- [36] S. M. Darbinian, K. A. Ispirian, and A. T. Margarian, *New mechanism for Unruh radiation of channeled particles*, Yerevan Physics Institute Preprint **65**, 1188 (1989).
- [37] P. A. M. Dirac, *Classical theory of radiating electrons*, Proceedings of the Royal Society of London. Series A. Mathematical and Physical Sciences **167**, 148 (1938).
- [38] L. Landau and E. M. Lifshitz, *The Classical Theory of Fields*, (Pergamon Press, Oxford, 1971).
- [39] A. Di Piazza, *Exact solution of the Landau-Lifshitz equation in a plane wave*, Letters in Mathematical Physics, **83**, 305 (2008).
- [40] Y. Hadad, L. Labun, J. Rafelski, N. Elkina, C. Klier, and H. Ruhl, *Effects of radiation reaction in relativistic laser acceleration*, Physical Review D **82**, 096012 (2010).
- [41] Y. Sheffer, Y. Hadad, M. H. Lynch, and I. Kaminer, *Towards precision measurements of radiation reaction*, arXiv:1812.10188 [physics.class-ph], (2018).
- [42] J. D. Jackson, *Classical Electrodynamics*, (John Wiley & Sons, New York, 1999).
- [43] D. S. Gemmell, *Channeling and related effects in the motion of charged particles through crystals*, Reviews of Modern Physics **46**, 129 (1974).
- [44] M. Tanabashi et al. (Particle Data Group), *Review of particle physics*, Physical Review D **98**, 030001 (2018).
- [45] A. A. Sokolov and I. M. Ternov, *Polarization and spin effects in the synchrotron radiation theory*, Doklady Akademii Nauk SSSR **153**, 1052 (1963).
- [46] J. S. Bell and J. M. Leinaas, *Electrons as accelerated thermometers*, Nuclear Physics B **212**, 131 (1983).
- [47] S.-Y. Lin and B. L. Hu, *Accelerated detector-quantum field correlations: From vacuum fluctuations to radiation flux*, Physical Review D **73**, 124018 (2006).
- [48] J. M. Cole et al., *Experimental evidence of radiation reaction in the collision of a high-intensity laser pulse with a laser-wakefield accelerated electron beam*, Physical Review X **8**, 011020 (2018).
- [49] K. Poder et al., *Experimental signatures of the quantum nature of radiation reaction in the field of an ultraintense Laser*, Physical Review X **8**, 031004 (2018).
- [50] P. R. Johnson and B. L. Hu, *Stochastic theory of relativistic particles moving in a quantum field: Scalar Abraham-Lorentz-Dirac-Langevin equation, radiation reaction, and vacuum fluctuations*, Physical Review D **65**, 065015 (2002).
- [51] P. R. Johnson and B. L. Hu, *Uniformly accelerated charge in a quantum field: from radiation reaction to Unruh effect*, Foundations of Physics **35**, 1117 (2005).

Acknowledgments

We would like to thank Niayesh Afshordi, Moti Segev, Jeff Steinhauer, and Germain Rousseaux for their valuable input and Tobias Wistisen for sending us the experimental data. E.C. acknowledges helpful discussions with the Bristol reading group regarding the Unruh effect. M.H.L. was supported in part at the Technion by a Zuckerman fellowship.

VI. SUPPLEMENTARY MATERIAL

A. The AQED Response Function

To begin our analysis we must first define the AQED response function. As we such, we examine electromagnetic emission in a refractive medium using the current interaction for QED

$$\hat{S}_I = \int d^4x \hat{j}_\mu(x) \hat{A}^\mu(x). \quad (\text{S1})$$

We shall couple an Unruh-DeWitt detector to the vector current. This will endow the electron an extra degree of freedom for energy transitions, i.e. the recoil. As such,

$$\hat{j}_\mu(x) = u_\mu \hat{q}(\tau) \delta^3(x - x_{tr}(\tau)). \quad (\text{S2})$$

The monopole moment operator $\hat{q}(t)$ is Heisenberg evolved via $\hat{q}(\tau) = e^{i\hat{H}\tau} \hat{q}(0) e^{-i\hat{H}\tau}$ with $\hat{q}(0)$ defined as $\hat{q}(0) |E_i\rangle = |E_f\rangle$ with E_i and E_f the initial energy and final energy of a two level system moving along the trajectory, $x_{tr}(t)$, of the current; transitions both up and down energy are allowed. With the intent to examine Larmor radiation, both in vacuum and an optical medium, we formulate the following amplitude;

$$\mathcal{A} = i \langle \mathbf{k} | \otimes \langle E_f | \hat{S}_i | E_i \rangle \otimes | 0 \rangle. \quad (\text{S3})$$

The differential probability per unit final state momenta is given by, $\frac{d\mathcal{P}}{d^3k} = |\mathcal{A}|^2$. Evaluation yields

$$\begin{aligned} \frac{d\mathcal{P}}{d^3k} &= |\langle \mathbf{k} | \otimes \langle E_f | \int d^4x \hat{j}_\mu(x) \hat{A}^\mu(x) | E_i \rangle \otimes | 0 \rangle|^2 \\ &= \int d^4x \int d^4x' |\langle E_f | \hat{j}_\mu(x) | E_i \rangle|^2 |\langle \mathbf{k} | \hat{A}^\mu(x) | 0 \rangle|^2. \end{aligned} \quad (\text{S4})$$

Note, the probability factorizes into an electron matrix element contracted with the photon matrix element. The electron matrix element yields

$$\begin{aligned} |\langle E_f | \hat{j}_\mu(x) | E_i \rangle|^2 &= |\langle E_f | u_\mu(x) e^{i\hat{H}\tau} \hat{q}(0) e^{-i\hat{H}\tau} \delta^3(x - x(\tau)) | E_i \rangle|^2 \\ &= q^2 U_{\mu\nu}[x', x] \delta^3(x - x_{tr}(\tau)) \delta^3(x' - x'_{tr}(\tau')) e^{-i\Delta E(\tau' - \tau)} \end{aligned} \quad (\text{S5})$$

Here we have defined the energy gap as $\Delta E = E_f - E_i$ and the charge as $q^2 = |\langle E_f | \hat{q}(0) | E_i \rangle|^2$. For the sake of brevity we defined a ‘‘velocity tensor’’ via $U_{\mu\nu}[x', x] = u_\nu(x') u_\mu(x)$. Next, we shall evaluate the photon inner product. For this we will need to integrate over the final state momenta, thereby developing the total emission probability. Hence,

$$\begin{aligned} \int d^3k |\langle \mathbf{k} | \hat{A}^\mu(x) | 0 \rangle|^2 &= \int d^3k \langle 0 | \hat{A}^{\dagger\nu}(x') | \mathbf{k} \rangle \langle \mathbf{k} | \hat{A}^\mu(x) | 0 \rangle \\ &= \langle 0 | \hat{A}^{\dagger\nu}(x') \hat{A}^\mu(x) | 0 \rangle \\ &= G^{\nu\mu}[x', x]. \end{aligned} \quad (\text{S6})$$

Note we have utilized the completeness relation, $\int dk |k\rangle \langle k| = 1$, to simplify the expression. The resultant is our photon two point function with vector indices. Using our photon two point function and the electron current density from Eqn. (S5). we can formulate the AQED response function $\frac{d\mathcal{P}}{d\eta} = \Gamma$. Hence

$$\begin{aligned} \mathcal{P} &= \int d^3k \int d^4x \int d^4x' |\langle E_f | \hat{j}_\mu(x) | E_i \rangle|^2 |\langle \mathbf{k} | \hat{A}^\mu(x) | 0 \rangle|^2 \\ \Rightarrow \Gamma &= q^2 \int d\xi e^{-i\Delta E \xi} U_{\mu\nu}[x', x] G^{\nu\mu}[x', x]. \end{aligned} \quad (\text{S7})$$

Here we have made use of the difference and average proptime change of variables; $\xi = \tau' - \tau$ and $\eta = (\tau' + \tau)/2$ respectively. Using the standard mode decomposition for the vector field in a dielectric medium, we have

$$\begin{aligned}\hat{A}^\mu(x) &= \int \frac{d^3k}{(2\pi)^{3/2}} \frac{\sum_i \epsilon_i^\mu}{\sqrt{n^2 2\omega}} \left[\hat{a}_k e^{i(\mathbf{k}\cdot\mathbf{x}-\omega t)} + \hat{a}_k^\dagger e^{-i(\mathbf{k}\cdot\mathbf{x}-\omega t)} \right] \\ &= \int \frac{d^3k}{(2\pi)^{3/2}} \frac{\sigma^\mu}{\sqrt{2\omega}} \left[\hat{a}_k e^{i(\mathbf{k}\cdot\mathbf{x}-\omega t)} + \hat{a}_k^\dagger e^{-i(\mathbf{k}\cdot\mathbf{x}-\omega t)} \right].\end{aligned}\quad (\text{S8})$$

Here we have the following standard dispersion relation $n\omega = k$, with index of refraction n . In the last line we have defined the quantity $\sigma^\mu = \frac{\sum_i \epsilon_i^\mu}{n}$. The two point function then reduces to an integral over the momentum,

$$\begin{aligned}\langle 0 | \hat{A}^{\dagger\nu}(x') \hat{A}^\mu(x) | 0 \rangle &= \langle 0 | \int \frac{d^3k'}{(2\pi)^{3/2}} \frac{\sigma'^{\dagger\nu}}{\sqrt{2\omega'}} \left[\hat{a}_{k'} e^{i(\mathbf{k}'\cdot\mathbf{x}'-\omega't')} + \hat{a}_{k'}^\dagger e^{-i(\mathbf{k}'\cdot\mathbf{x}'-\omega't')} \right] \\ &\quad \times \int \frac{d^3k}{(2\pi)^{3/2}} \frac{\sigma^\mu}{\sqrt{2\omega}} \left[\hat{a}_k e^{i(\mathbf{k}\cdot\mathbf{x}-\omega t)} + \hat{a}_k^\dagger e^{-i(\mathbf{k}\cdot\mathbf{x}-\omega t)} \right] | 0 \rangle \\ &= \frac{1}{(2\pi)^3} \frac{1}{2} \int \frac{d^3k}{\omega} \sigma^\mu \sigma'^{\dagger\nu} e^{i(\mathbf{k}\cdot\Delta\mathbf{x}-\omega(t'-t))}.\end{aligned}\quad (\text{S9})$$

Again we see that the vector two point function is formally the same as a scalar field but with polarization vectors lending their indices. Combining all the pieces we can formulate the response function for our photon emission.

$$\Gamma = q^2 \frac{1}{(2\pi)^3} \frac{1}{2} \int d\xi \int \frac{d^3k}{\omega} U e^{-i(\Delta E \xi - \mathbf{k}\cdot\Delta\mathbf{x}_{tr} + \omega \Delta t)}.\quad (\text{S10})$$

We defined the velocity product $U = \sigma^\mu \sigma'^{\dagger\nu} U_{\mu\nu}[x', x]$ for brevity. Let us now examine the power radiated by a uniformly accelerated charge.

B. The Thermalized Vacuum Larmor Formula

To analyze Larmor emission we will now consider the electron propagating in free space, i.e. $n = 1$. We will begin by examining the polarization vectors that are contracted with our velocity tensor. Recalling that under proper acceleration a , the four-velocities at proper time τ will be given $u^\mu = (\cosh(a\tau), 0, 0, \sinh(a\tau))$. Hence,

$$\begin{aligned}U &= \left(\sum_i u_\mu \epsilon_i^\mu \right) \left(\sum_j u_\nu \epsilon_j^\nu \right)^\dagger \\ &= \left(\sum_i \mathbf{u} \cdot \epsilon_i \right) \left(\sum_j \mathbf{u}' \cdot \epsilon_j \right)^\dagger \\ &= \sinh(a\tau) \sinh(a\tau') \sin^2(\theta).\end{aligned}\quad (\text{S11})$$

Here θ is the angle of photon emission relative to the direction of propagation along the z -axis. Moreover we will make use of the hyperbolic double angle formulas to obtain

$$\sinh(a\tau) \sinh(a\tau') = \frac{1}{2} [2 \cosh^2(a\eta) - 1 - \cosh(a\xi)].\quad (\text{S12})$$

Combining all the above pieces we can now formulate the transition probability. Thus

$$\Gamma = q^2 \frac{1}{(2\pi)^3} \frac{1}{4} \int d\xi \int \frac{d^3k}{\omega} [2 \cosh^2(a\eta) - 1 - \cosh(a\xi)] \sin^2(\theta) e^{-i(\Delta E \xi - \mathbf{k}\cdot\Delta\mathbf{x}_{tr} + \omega \Delta t)}.\quad (\text{S13})$$

To arrive at the Larmor formula, typically computed in the rest frame of the electron, we must make use of the nonrelativistic approximation; $\Delta x \sim 0$ and note that with respect to the variable η , the Lorentz gamma is given by $\gamma = \cosh(a\eta)$ which we also take to be 1. As such we obtain

$$\Gamma = q^2 \frac{1}{(2\pi)^3} \frac{1}{4} \int d\xi [1 - \cosh(a\xi)] \int \frac{d^3k}{\omega} \sin^2(\theta) e^{-i(\Delta E\xi + \omega\Delta t)}. \quad (\text{S14})$$

Now, examining the momentum integrations, we move to spherical coordinates with the momentum aligned along the z-axis, to yield

$$\begin{aligned} \Gamma &= q^2 \frac{1}{(2\pi)^3} \frac{1}{4} \int d\xi [1 - \cosh(a\xi)] \int d\theta d\omega d\phi \omega \sin^3(\theta) e^{-i(\Delta E\xi + \omega\Delta t)} \\ &= \frac{2}{3} \alpha \frac{1}{2\pi} \int d\xi [1 - \cosh(a\xi)] \int d\omega \omega e^{-i(\Delta E\xi + \omega\Delta t)} \end{aligned} \quad (\text{S15})$$

Note, in the last line we rewrote the prefactor in terms of the fine structure constant $\alpha = \frac{q^2}{4\pi}$. To compute the Larmor formula, we will need to examine the power emitted by the photon. As such we weight the frequency integral with an additional factor of frequency. Hence

$$\mathcal{S} = \frac{2}{3} \alpha \frac{1}{2\pi} \int d\xi e^{-i\Delta E\xi} [1 - \cosh(a\xi)] \int d\omega \omega^2 e^{-i\omega\Delta t}. \quad (\text{S16})$$

The integration over the frequency can now be carried out to yield

$$\int d\omega \omega^2 e^{-i\omega\Delta t} = \frac{2i}{\Delta t^3}. \quad (\text{S17})$$

We should note that there is an implicit regulator $\Delta t \rightarrow \Delta t - i\epsilon$ in the denominator. This will later require us to include a pole on the real axis in the integration over the proper time. Our integration now simplifies to

$$\mathcal{S} = \frac{2}{3} \alpha \frac{i}{\pi} \int d\xi e^{-i\Delta E\xi} \frac{[1 - \cosh(a\xi)]}{\Delta t^3}. \quad (\text{S18})$$

Finally we recall that $\Delta t = \frac{2}{a} \sinh(a\xi/2)$, we have

$$\mathcal{S} = \frac{2}{3} \alpha \frac{i}{\pi} \left(\frac{a}{2}\right)^3 \int d\xi e^{-i\Delta E\xi} \frac{[1 - \cosh(a\xi)]}{\sinh^3(a\xi/2)}. \quad (\text{S19})$$

Converting the hyperbolic terms to exponentials and making the change of variables $w = e^{a\xi}$, we have

$$\mathcal{S} = \frac{2}{3} \alpha \frac{i}{\pi} \left(\frac{a}{2}\right)^3 \frac{8}{a} \int dw \frac{[w^{1/2 - i\Delta E/a} - \frac{1}{2}w^{3/2 - i\Delta E/a} - \frac{1}{2}w^{-1/2 - i\Delta E/a}]}{[w - 1]^3}. \quad (\text{S20})$$

This integration is standard and can be evaluated using the residue theorem. As such we obtain the following

$$\mathcal{S} = \frac{2}{3} \alpha a^2 \frac{1}{1 + e^{2\pi\Delta E/a}}. \quad (\text{S21})$$

This is our thermal Larmor formula. By summing over transitions both up and down in energy, i.e. when $\Delta E = |\Delta E|$ and $\Delta E = -|\Delta E|$, and taking the limit $|\Delta E| \rightarrow 0$ we arrive at the standard Larmor formula. Hence

$$\mathcal{S} = \frac{2}{3} \alpha a^2. \quad (\text{S22})$$

Note, this is written in terms of the proper acceleration and therefore is fully relativistic as in the classical derivation. Now that we have verified our method of computation, let us compute the power spectrum in a refractive medium.

C. Power Spectrum

Prior to integrating over the emitted photons frequency, Eqn. (S14), we will have the following emission rate

$$\Gamma = q^2 \frac{1}{(2\pi)^3} \frac{1}{4} \int d\xi \int \frac{d^3k}{\omega} [2 \cosh^2(a\eta) - 1 - \cosh(a\xi)] \sin^2(\theta) e^{-i(\Delta E \xi - \mathbf{k} \cdot \Delta \mathbf{x}_{tr} + \omega \Delta t)}. \quad (\text{S23})$$

We will further simplify by using the following redefinition $\delta = 2\gamma^2 - 1$. Utilizing the same approximation $\Delta x \sim 0$, which reproduces the Larmor formula, but now keeping our boost parameter, which is a function of η only, we can now convert to spherical coordinates and integrate over the emission angle. Hence

$$\begin{aligned} \Gamma &= q^2 \frac{1}{(2\pi)^3} \frac{1}{4} \int d\xi \int \frac{d^3k}{\omega} [\delta - \cosh(a\xi)] \sin^2(\theta) e^{-i(\Delta E \xi + \omega \Delta t)} \\ &= q^2 \frac{1}{(2\pi)^2} \frac{1}{3} \int d\xi \int d\omega \omega [\delta - \cosh(a\xi)] e^{-i(\Delta E \xi + \omega \Delta t)} \end{aligned} \quad (\text{S24})$$

weighting by an extra factor of frequency to obtain the power, we formulate the power spectrum, $\frac{d\mathcal{P}}{d\omega}$. Hence

$$\frac{d\mathcal{P}}{d\omega} = q^2 \frac{1}{(2\pi)^2} \frac{1}{3} \int d\xi \omega^2 [\delta - \cosh(a\xi)] e^{-i(\Delta E \xi + \omega \Delta t)} \quad (\text{S25})$$

Recalling that with the boost parameter, $\Delta t = \frac{2}{a} \sinh(a\xi/2)\gamma$, we now convert hyperbolic cosine to exponentials to obtain

$$\begin{aligned} \frac{d\mathcal{P}}{d\omega} &= q^2 \frac{1}{(2\pi)^2} \frac{\omega^2}{3} \int d\xi \left[\begin{aligned} &\delta e^{-i(\Delta E \xi + \frac{2\omega\gamma}{a} \sinh(a\xi/2))} \\ &- \frac{1}{2} e^{-i((\Delta E + ia)\xi + \frac{2\omega\gamma}{a} \sinh(a\xi/2))} \\ &- \frac{1}{2} e^{-i((\Delta E - ia)\xi + \frac{2\omega\gamma}{a} \sinh(a\xi/2))} \end{aligned} \right]. \end{aligned} \quad (\text{S26})$$

Employing the change of variables $w = a\xi/2$ we obtain

$$\begin{aligned} \frac{d\mathcal{P}}{d\omega} &= q^2 \frac{1}{(2\pi)^2} \frac{\omega^2}{3} \frac{2}{a} \int dw \left[\begin{aligned} &\delta e^{(-\frac{2i\Delta E}{a} w - \frac{2i\omega\gamma}{a} \sinh(w))} \\ &- \frac{1}{2} e^{(-(\frac{2i\Delta E}{a} - 2)w - \frac{2i\omega\gamma}{a} \sinh(w))} \\ &- \frac{1}{2} e^{(-(\frac{2i\Delta E}{a} + 2)w - \frac{2i\omega\gamma}{a} \sinh(w))} \end{aligned} \right]. \end{aligned} \quad (\text{S27})$$

Now, recalling the integral representation of the second Hankel function, we have

$$H_n^{(2)}(x) = -\frac{1}{i\pi} \int_{-\infty}^{\infty - i\pi} dt e^{-nt + x \sinh(t)}. \quad (\text{S28})$$

Here, the integration contour is shifted down by $-\pi$ on the imaginary axis. This is consistent with the Larmor case since there we used our $\Delta t - i\epsilon$ prescription. Using the above formula we find our power spectrum to be

$$\frac{d\mathcal{P}}{d\omega} = -i \frac{2}{3} \alpha \frac{\omega^2}{a} \left[\delta H_{\frac{2i\Delta E}{a}}^{(2)} \left(-\frac{2i\omega\gamma}{a} \right) - \frac{1}{2} \left(H_{\frac{2i\Delta E}{a} - 2}^{(2)} \left(-\frac{2i\omega\gamma}{a} \right) + H_{\frac{2i\Delta E}{a} + 2}^{(2)} \left(-\frac{2i\omega\gamma}{a} \right) \right) \right]. \quad (\text{S29})$$

To make the presence of thermality more apparent, we make use of the following identity, $H_\ell^{(2)}(x) = e^{i\ell\pi} H_{-\ell}^{(2)}(x)$. As such, each term will yield precisely a Boltzmann factor with the Unruh-DeWitt detector energy gap thermalized at the celebrated Fulling-Davies-Unruh temperature. Applying this identity then yields our power spectrum,

$$\frac{d\mathcal{P}}{d\omega} = -i\frac{2}{3}\alpha\frac{\omega^2}{a}e^{-2\pi\Delta E/a} \left[\delta H_{-\frac{2i\Delta E}{a}}^{(2)}\left(-\frac{2i\omega\gamma}{a}\right) - \frac{1}{2} \left(H_{-\frac{2i\Delta E}{a}+2}^{(2)}\left(-\frac{2i\omega\gamma}{a}\right) + H_{-\frac{2i\Delta E}{a}-2}^{(2)}\left(-\frac{2i\omega\gamma}{a}\right) \right) \right]. \quad (\text{S30})$$

This power spectrum contains the Unruh-DeWitt detector energy gap thermalized at the Fulling-Davies-Unruh temperature. Let us now explore the use of radiative energy loss, as a source for acceleration. We will then compare our results with the recent experimental observation of radiation reaction in aligned crystals.

D. Acceleration via Radiative Energy Loss

To apply the above formalism to the recent experiments we must first look at the acceleration. Assuming a model of based on radiative energy loss, we have

$$\begin{aligned} \frac{dE}{dx} &= -\frac{E}{x_0} \\ \Rightarrow E(x) &= E_0 e^{-x/x_0}. \end{aligned} \quad (\text{S31})$$

The parameter x_0 is the radiation length and determines the distance traversed in medium until the particle losses e^{-1} of its initial energy. Let us consider an ultra-relativistic particle and assume the initial energy will be entirely due to the momentum mu_0 , with u_0 being the initial proper velocity. This expression gives the proper velocity as a function of distance in the lab frame. Thus,

$$u(x) = u_0 e^{-x/x_0}. \quad (\text{S32})$$

This expression can be used to determine the distance traveled in the laboratory as a function of proper time. Hence

$$\begin{aligned} \frac{dx}{d\tau} &= u_0 e^{-x/x_0} \\ \Rightarrow x(\tau) &= x_0 \ln(\tau/\tau_0 + 1). \end{aligned} \quad (\text{S33})$$

Here, $\tau_0 = x_0/u_0$, and we have fixed our boundary condition at $x(\tau = 0) = 0$. To determine the proper velocity and acceleration all we need to do is differentiate. Hence

$$\begin{aligned} u(\tau) &= \frac{u_0}{\left(\frac{\tau}{\tau_0} + 1\right)} \\ a(\tau) &= \frac{a_0}{\left(\frac{\tau}{\tau_0} + 1\right)^2}. \end{aligned} \quad (\text{S34})$$

Note we have taken the magnitude of the acceleration. The overall scale of the acceleration is given by $a_0 = u_0/x_0$ which depends on the material as well as the initial energy. For ultra-relativistic velocities we have $u_0 \sim \gamma_0 = E_0/m$. The other kinematic factors that we need to describe our system are given by:

$$\begin{aligned} a_0 &= \frac{\gamma_0}{x_0} \\ \tau_0 &= \frac{x_0}{\gamma_0}. \end{aligned} \quad (\text{S35})$$

Note that all relevant parameters that are written in terms of the particle energy, mass, and the radiation length of the material. For the crystal experiment, the relevant energy scale is GeV. For positrons, silicon will have a radiation length of $x_0 = 9.37$ cm. For the experiment in question we have the following parameters;

$$\begin{aligned}
x_0 &= 4.75 \times 10^{14} \text{ GeV}^{-1} \\
E_0 &= 178.2 \text{ GeV} \\
m &= .000511 \text{ GeV}.
\end{aligned}
\tag{S36}$$

To model the energy gap we use the following parameterization,

$$\Delta E = a_0 + a_1\omega + a_2\omega^2 + a_3\omega^3. \tag{S37}$$

For the current analysis, we note that constant term will be determined by the channeling frequency and the second order term will encode phenomena such as recoil. To match the calculated spectrum to the data for both bremsstrahlung and the aligned crystal case we also include an over all scaling factor s for the spectrum and also scale the radiation length by a factor of \tilde{x} to take into account any additional phenomena that may occur and contribute to the energy loss.

| Crystal | Energy | Gap | χ^2/ν | s | \tilde{x} | a_0 [GeV] | a_1 | a_2 [GeV ⁻¹] | a_3 [GeV ⁻²] |
|-----------------|--------|-----|--------------|--------|-------------|-------------|---------|----------------------------|----------------------------|
| 3.8 mm Aligned | 30 GeV | No | 4.187 | 6.524 | 2.7998 | 0 | 0 | 0 | 0 |
| 3.8 mm Aligned | 30 GeV | Yes | 1.114 | 12.93 | 3.9231 | -0.00197 | 0.0120 | -846.2 | 0.4691 |
| 10 mm Amorphous | 40 GeV | No | 1.517 | 0.2134 | 1.9381 | 0 | 0 | 0 | 0 |
| 10 mm Amorphous | 40 GeV | Yes | 1.065 | 0.3398 | 2.4820 | 0.0148 | -0.0198 | -400.73 | -1.0729 |

TABLE S1: The best fit parameters for our theoretical power spectrum both with and without the energy gap for the 3.8 mm channeling and 10 mm bremsstrahlung crystal samples at the energy where the chi-squared statistic first meets the 1 standard deviation criterion. Our reduced chi-squared statistics shows that the data can be rigorously fit by the power spectrum with the energy gap thermalized at the FDU temperature.